

Hydrodynamic Simulation of Rip Currents Along Al-Nakheel Beach, Alexandria, Egypt: Case Study

Nada M. Salama¹, Moheb M. Iskander², Ahmed A. El-Gindy¹, Abdallah M. Nafeih¹ and Hossam El-Din M. Moghazy³

Received: 12 May 2022 / Accepted: 16 October 2022

© Harbin Engineering University and Springer-Verlag GmbH Germany, part of Springer Nature 2023

Abstract

Al-Nakheel beach is located northwest of Alexandria city, Egypt, along the Mediterranean coast. During the period from 1998 to 2003, seven detached breakwaters were constructed along Al-Nakheel beach to create a sheltered area for swimming. Unfortunately, the structures amplify rip currents, shoreline accretions, and erosions. The aim of this research is to track the variations of the rip currents within the study area and show the effects of the breakwaters on the shoreline. The research is based on the hydrodynamic and morphological data of the study area and uses the Delft3D hydrodynamical model combined with other data analysis tools to serve the model input. The data include measured sea-level observations in 2013, the ERA-interim wave datasets from 2015 to 2018 and wind data in 2018, bed morphologies, and Google Earth satellite images from 2010 to 2020. The model is calibrated on the basis of the available current measurements within the nearshore zone. Results show that the shoreline eroded at an average rate of about 0.9 m/yr. Moreover, pairs of vortices are formed behind the breakwaters with an average current velocity of 0.6 m/s. The predominant northwest waves induce rip currents on the leeside of the structures with velocities reaching 1.2 m/s, associated with the rip pulsation that extends offshore. The problem solution decision recommends the removal of the sand deposition on the leeside of the breakwaters by an average amount of 100 000 m³/yr and the fencing of the safe area for swimming by a floating fence of 1 000 m length and 65 m average width.

Keywords Nearshore process; Rip current; Al-Nakheel beach; Delft3D model

1 Introduction

Monitoring hotspots of rip currents along beaches that are teeming with people is a global challenge. A rip current is

a local, powerful, seaward-directed, jet-like stream that forms in the surf zone and spreads outside the breaking zone. For beachgoers, a rip current velocity of less than 0.2 m/s is considered safe. However, typical rip current velocities range from 0.3 m/s to 1.0 m/s, with some cases exceeding 2.0 m/s, which are considered dangerous for swimmers (Benassai et al. 2017; Castelle et al. 2016; Dudkowska et al. 2020; Iskander et al. 2021; Short 1985). In general, a rip is nominated as a “mega rip” if the rip current extends offshore twice the distance of the surf zone (Leatherman 2012). Rip currents are divided into three categories. Hydrodynamically controlled rips appear on beaches with consistent bathymetry along shores and are temporally and spatially transitory. Morphologically controlled rip currents are induced by bathymetric changes and alongshore hydrodynamic fluctuations; this category is quasi-permanent in space and time (Gallop et al. 2018). Boundary-controlled rip currents (structurally controlled) can be encountered where perpendicular rigid structures are regulated naturally or artificially (Castelle and Coco 2013).

Every year, rip currents cause hundreds of rescues and

Article Highlights

- The consequences of the construction of beach protective structures such as breakwaters along Al-Nakheel beach;
- The problem solution decision recommends dredging the salient formed on the leeside of the detached breakwaters and constructing a floating fence.

✉ Nada M. Salama
Nada.salama_PG@alexu.edu.eg

¹ Department of Oceanography, Alexandria University, Alexandria 21526, Egyptian

² Department of Hydrodynamics, Coastal Research Institute, Alexandria 21514, Egyptian

³ Department of Irrigation Engineering and Hydraulics, Alexandria University, Alexandria 21544, Egyptian

deaths on beaches everywhere in the world. Previous reports mentioned that in 2017, about 1074 drowning cases were recorded along the Egyptian Mediterranean coast (Roth 2018).

The northwest coast of Egypt suffers from moderate risk rip currents, especially during spring and summer (Iskander et al. 2021). The northwestern coast of Egypt, including the study area, is regarded as a moderately dissipative beach. Rip currents are also typically associated with intermediate-level beaches (Wright and Short 1984). Al-Nakheel breakwaters have induced the rip formation and enhanced its velocity-forming vortices. Al-Nakheel is considered one of the hotspots for the rip current generation in Egypt. The Egyptian government has decided to close Al-Nakheel beach and prevent swimming within this beach to save beachgoers' lives. This study aims to suggest how to control the rip current problem of Al-Nakheel beach.

The study area extends over 1000 m between latitudes 31.096 2°N and 31.074 8°N and longitudes 29.706°E and 29.739 3°E, as shown in Figure 1. Al-Nakheel beach is considered one of the main recreational beaches along the northwest coast of Egypt. Iskander et al. (2007) reported that to provide a safe area for swimming in “Al-Nakheel beach” seven detached breakwaters were constructed in front of “Al-Nakheel beach” between 1998 and 2003. Each breakwater is protected by dolos armor layers and measures 100 m long, +1.0 m above mean sea level, 200 m from the shoreline, and 50 m gap from the neighboring breakwater. The seven breakwaters front a shoreline of about 1.0 km long. A small temporary harbor was built west of the construction area to provide supplies, but after the construction process, the harbor was removed. Morphologic changes were detected behind the detached breakwaters. The shoreline changes were detected between 20 and 70 m on the low-energy leeside of the structure (Iskander et al. 2007).

EPADP (2019) reported that the western Nubaria drain has a total length of about 68400 m. Two straight jetties of 65 m each, consisting of stone armor layers, were constructed at the exit of the drain in 1986 to protect and stabilize it from siltation. The bottom width is about 6 m, and the total discharge rate is 63 m³/s.

2 Materials and data

2.1 Bathymetry

The shoreline used in the bathymetric map was obtained

using Google Earth images, as shown in Figure 1. The water depth was determined using a contour map of 2019 based on a nautical chart produced by the Egyptian Navy Hydrographic Department (ENHD) (Khedr 2019). This nautical chart (INT-3553) in 2002 was obtained under a framework of a project implemented by the Oceanography Department at the Faculty of Science, Alexandria University, as presented in Table 1. The shoreline and the corresponding water depth overlapped and were used in building the hydrodynamical model.

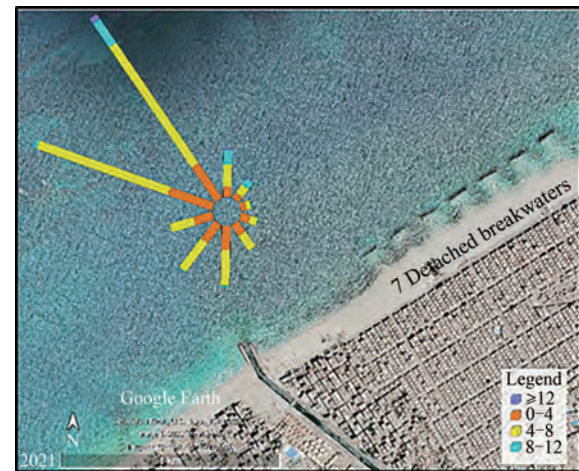


Figure 1 The study area, as displayed in Google Earth's image of 2021, shows the seven detached breakwaters and the western Nubaria drain. The wind rose in 2018, and the coloured legend of the wind speed in m/s was implemented during this research

2.2 Wave data

The wave data (significant wave heights, corresponding periods, and directions) were downloaded from the European Center for Medium-range Weather Forecasts (ECMWF) ERA-interim database for 48 months from January 2015 to December 2018. The dataset was downloaded for three stations, as shown in Table 2. The distance between each of the two northward successive stations was 14 km.

2.3 Wind data

Wind data (components u and v) for 12 months (January–December 2018) were downloaded from (ECMWF) ERA-interim database. The dataset was downloaded for three stations, as presented in Table 2. The distance between each of the two northward successive stations was 14 km. The

Table 1 Bathymetry data used in the current study

Data	Source	Year	Region (Egypt)
Shoreline	Google Earth	2010 2020	El-Burullus to El-Dabaa
Bathymetry	Nautical chart (INT-3553)	2002	El-Agami to Sidi Krir
Bathymetry	Nautical chart (Khedr 2019)	2019	El-Agami to Sidi Krir

Table 2 Data used in the current study where stations 1 (St-1), 2 (St-2), and 3 (St-3) are at 200, 40, and 10 m depths, respectively

Dataset	Period	Temporal resolution	Latitude and longitude
Wave (St-1)	2015	6 h	31°15'0"N 29°30'0"E
	2016		
	2017		
	2018		
Wave (St-2)	2015	6 h	31°07'30"N 29°30'0"E
	2016		
	2017		
	2018		
Wave (St-3)	2015	6 h	31°0'0"N 29°30'0"E
	2016		
	2017		
	2018		
Wind (St-1)	2018	3 h	31°15'0"N 29°30'0"E
Wind (St-2)	2018	3 h	31°07'30"N 29°30'0"E
Wind (St-3)	2018	6 h	31°0'0"N 29°30'0"E
Sea level (SL)	2013	30 min	31°11'56"N 29°52'21"E

following equations were applied to calculate the wind speed (Equation (1)) and the wind direction (Equation (2)) according to (Nelson 1984). The wind speed ω is expressed in (m/s), u is the east component, and v is the north component. The wind direction Φ is related to an angle from which the wind is blowing relative to the north.

$$\omega = \text{sqrt}(u^2 + v^2) \quad (1)$$

$$\Phi = \begin{cases} \tan^{-1} \frac{u}{v} & \text{for the first quadrant} \\ \tan^{-1} \frac{v}{u} + 90^\circ & \text{for the second quadrant} \\ \tan^{-1} \frac{u}{v} + 180^\circ & \text{for the third quadrant} \\ \tan^{-1} \frac{v}{u} + 270^\circ & \text{for the forth quadrant} \end{cases} \quad (2)$$

2.4 Sea-level data

Sea-level variations were recorded at Alexandria western harbor in 2013. The dataset was recorded using an aqua pressure sensor tide gage deployed at 3 m below mean sea level (Khedr 2019), acquired by ENHD, as displayed in Table 3.

Table 3 Significant tidal components from the measured data of 2013 in the study area

Tide component	Name	Phase (°)	Amplitude (cm)
O1	Principal lunar elliptic	289	1.26
P1	Principal solar diurnal	326	0.56
K1	Lunisolar diurnal	319	1.7
OO1	Lunar diurnal	305	0.22
N2	Larger lunar elliptic	331	1.12
M2	Principal lunar	332	6.72
L2	Smaller solar elliptic	345	0.41
S2	Principal solar	347	4.1
K2	Lunisolar semidiurnal	343	1.26
M3	Lunar terdiurnal constituent	9	0.15

3 Method

3.1 Detection of coastal hydrodynamic basic processes

Wave climate was studied through the spatial comparison of monthly mean wave parameters, from the offshore area getting through (St-1) to the nearshore getting through (St-3), using the three-year dataset (2015–2018). In addition, the wind attributes over the study area expressed through the wind rose in 2018. Moreover, the harmonic analysis was applied to sea-level observations using (t-tide) to obtain the tidal components where they were used as the boundary conditions in the hydrodynamic model. Eight Google Satellite images were used to detect the shoreline change during the period from 2010 to 2020.

3.2 Coupling between Delft3D wave module and Delft3D flow

The wave module is based on the third-generation wave module (SWAN), which was developed by Delft University of Technology. The prognostic equation of the model is the wave action, N , balance equation (Booij et al. 1999; Holthuijsen 2007). SWAN is a well-known spectral wave model that solves the transport equation without any restrictions on the spectrum shape of wave energy. The model includes important processes, such as wind input, dissipation, and nonlinear wave interaction. Furthermore, SWAN calculates wave propagation from deep water to the surf zone. Source and sink terms are influenced by six processes.

The term $S(\sigma, \theta_\omega, x, y, z)$ represents the source and sink components

$$S(\omega, \theta_\omega) = S_{\text{in}}(\omega, \theta_\omega) + S_{nl4}(\omega, \theta_\omega) + S_{nl3}(\omega, \theta_\omega) + S_{\text{ocap}}(\omega, \theta_\omega) + S_{\text{bot}}(\omega, \theta_\omega) + S_{\text{br}}(\omega, \theta_\omega) \quad (3)$$

where S_{in} denotes the wave growth as a result of the wind input. The nonlinear transmission of wave energy through three- and four-wave interactions is represented by the second and third components, respectively. The last three terms, white capping, bottom friction, and depth-induced wave breaking, represent wave decay and dissipation.

3.3 Model setup and simulation scenarios

3.3.1 Bathymetry

The bathymetric dataset was digitized from the Admiralty charts that had been spatially georeferenced and corrected. A detailed bathymetry was obtained, as illustrated in Figure 2. The dataset was subjected to triangular interpolation and smoothing in the Delft3D Quicken suite and defined as depth.

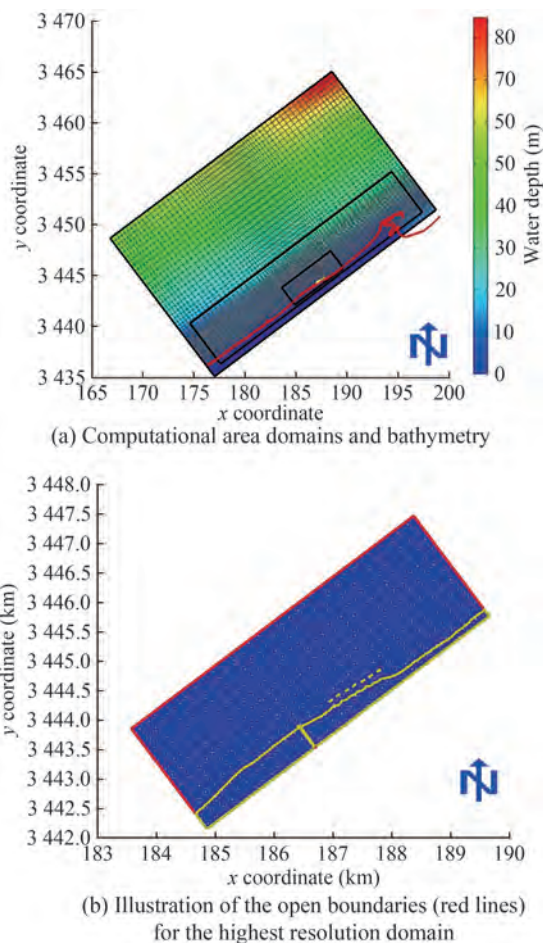


Figure 2 Illustration of the model setup

3.3.2 Computational domains

Initially, the SWAN approach was developed on nested domains, as displayed in Figure 2(a). On a coarse grid of an average 150 m resolution, the model was first utilized to simulate wave propagation over the region of 27 km wide and 16 km offshore. Furthermore, detailed grids were

created by nesting to simulate wave propagation. A grid with a resolution of 50 m was built for an area of 24 km in width and 5 km offshore. Moreover, a grid with a resolution of 10 m was developed for an area of 5 km along the shoreline and 2 km offshore to simulate wave propagation within the structure area. The same resolution was used in the flow model.

3.3.3 Scenarios

The coupling between modules was developed for five simulation scenarios, considering a specific selection for the types of open boundaries, as illustrated in Figure 2(b). Seeking to detect the effects of the detached breakwaters on rip current behaviors along Al-Nakheel beach, the simulation scenarios were designed as follows:

a) Scenario 1 depicts the present case of Al-Nakheel beach, where seven detached breakwaters exist, considering the water bathymetry in 2019 (Khedr 2019).

b) Scenario 2 shows the area where no breakwaters exist, considering the straight shoreline in 1998, water bathymetry modified from the 2002 map, and the flow of the western Nubaria drain (60 m³/s).

c) Scenario 3 is a suggestion to manipulate the shoreline mentioned in (SPA 2018) and (Iskander et al. 2021) by removing the tombolo or salient accretion formed on the leeside of these structures. The salient accretions convert the shoreline from a straight to a cusped shape, which, in turn, helps in rip current formation (Leatherman 2012).

d) Scenario 4 is a trial to merge the manipulated shoreline and decrease the discontinuity of breakwaters to exhibit the effects of decreasing gaps on rip production.

e) Scenario 5 is the present case of Al-Nakheel beach but without the flow of the drain.

3.3.4 Model calibration

Williams and Esteves (2017) reported that the model calibration procedure involves a comparison of predictions and observations. According to Elkut et al. (2021), calibration considers temporal and spatial factors. The calibration of the flow model in the present study was evaluated using the observed current data during a two-year period (2002–2004). The data were measured at two locations: El-Nubaria (31°5.258'N and 29°42.833'E) and El-Agami (31°7.445'N and 29°46.097'E), as reported by (Iskander 2008). The results indicate that at El-Nubaria and El-Agami stations, the maximum current velocities reached 0.4 and 0.5 m/s, and the average current velocities were 0.27 and 0.31 m/s, respectively. The predicted current speed was close to the measured data at El-Agami and El-Nubaria stations, with a percentage prediction error range between 7.3% and 7.4%.

The performance of the flow module with high-resolution domains, considering all factors, bed morphologies, coastal processes, and beach orientation from the true north, can simulate the study area with acceptable accuracy.

4 Results and discussion

4.1 Basic coastal hydrodynamic

One of the principal forces on the beach is waves, which are mostly generated by winds in the offshore area. The nearshore current system is also influenced by waves. In addition, wave height, incident wave effective angle, and average coastline orientation influence longshore and rip current direction and magnitude. Analyzing the available wave data from 2015 to 2018 shows that the significant wave height (H_s) in the study area ranges from 0.5 m to 1.4 m most of the year, as illustrated in Figure 3(a). The maximum wave heights offshore and nearshore are 5.1 and 4.4 m, respectively, which agrees with (Iskander et al. 2013). The shoaling effect is obvious when comparing maximum wave heights from offshore to nearshore stations. Furthermore, H_s in winter months is higher than in summer months. A minor change in the wave period is remarkable from (St-1) to (St-3), as shown in Figure 3(b). The wave periods range between 4 and 6 s most of the year. The maximum wave period is about 10 s. The most dominant wave direction is northwest as shown in Figure 3(c), where they reach perpendicular to the shoreline. Such a climate is in accordance with (Salama 2021) and Iskander et al. (2013). The most dominant wind direction in 2018 is from the west-northwest, and the wind speed varies between 4 and 8 m/s.

The harmonic analysis result of the 2013 tide data reveals two significant tidal energies that occur in diurnal and semidiurnal bands (0.04 cph = 25 h and 0.08 cph = 12.5 h). The main type of tidal cycle is the semidiurnal tide. The most effective and significant tidal components are the principal lunar (M2) and solar (S2) constituents, as presented in Table 3. The amplitude and phase angle of (M2) are in accordance with (Mosetti and Purga 1990). The (S2) result agrees with (Moursy 1996).

The shoreline change study from 2010 to 2020 indicates that sand deposited from the original shoreline to barriers is allowed by detachable breakwaters, forming “saliency,” as illustrated in Figures 4(a), (b). Given that the sediment transport process is in balance, erosion zones are formed among the formed salients, according to (Ciarmiello and Natale, 2016). The shoreline is eroded at an average rate of 0.9 m/yr from 2010 to 2020. Except in the zone at the fifth cross profile (CP5), different signs in the calculations express an inverse process to erosion, where a deposition exists at a rate of 0.5 m/yr, which is in agreement with (Iskander 2021).

4.2 Simulation scenarios and flow patterns

4.2.1 Simulation of the present situation of Al-Nakheel beach (Scenario 1)

This scenario exhibits the current situation at Al-Nakheel beach, where coupling between flow and SWAN modules is running simultaneously. All conditions of the beach are

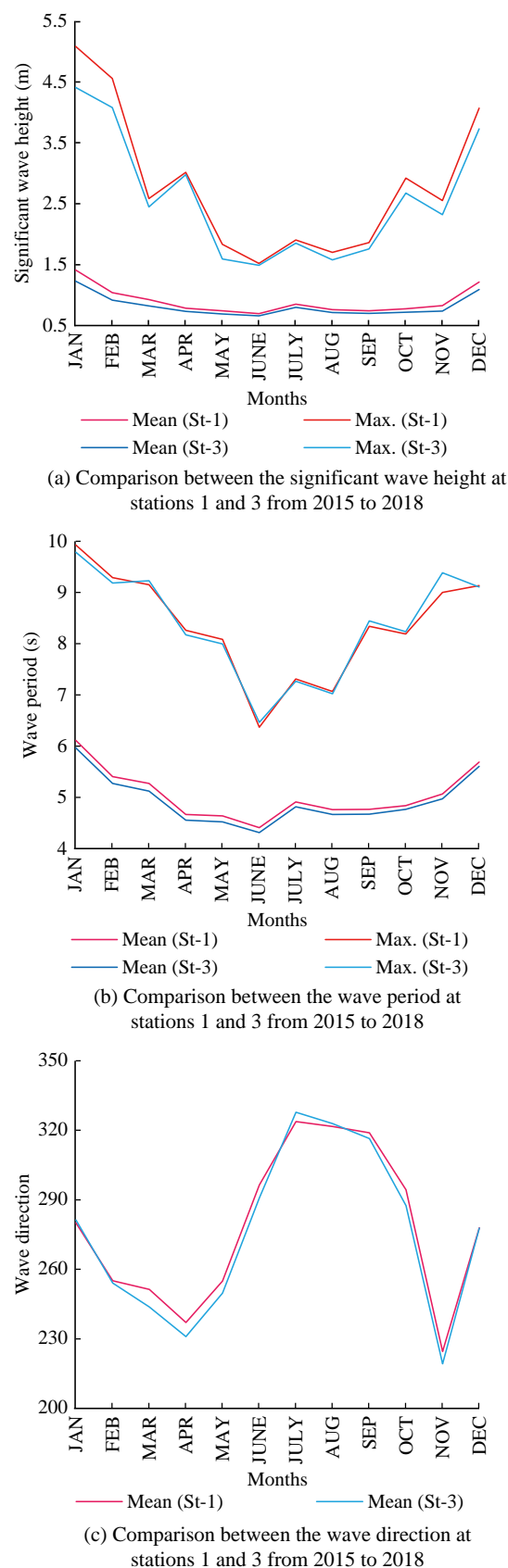


Figure 3 Comparison between the wave climate at stations 1 and 3 from 2015 to 2018

considered (recent shoreline and bathymetry, the seven detached breakwater dimensions, interspaces and distances from the shoreline, and flow from the western Nubaria drain). The wave and wind characteristics (wave height, wave period, wave direction, wind speed and direction) for this scenario in 2018 are captured. The boundary conditions are

selected, as shown in Figure 2(b).

The outcome is wave-induced rip current formation, as illustrated in Figure 5. The most dominant wave climate, resulting in the rip current formation, is the west-northwest waves that come perpendicular to the shoreline, as shown in Figure 5(c). The breakwaters reduce the wave height but

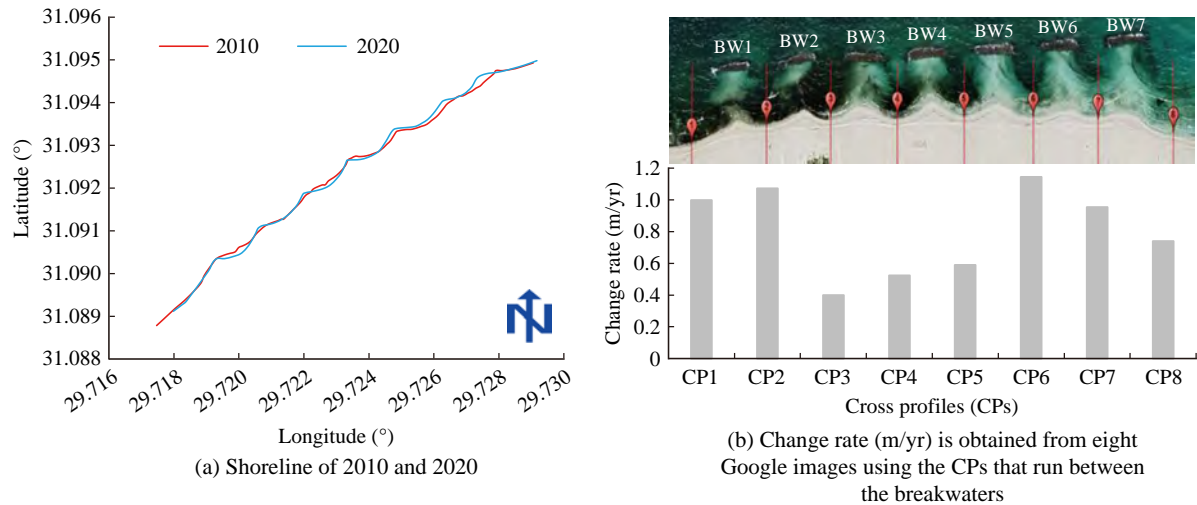


Figure 4 Shoreline changes along Al-Nakheel beach from 2010 to 2020

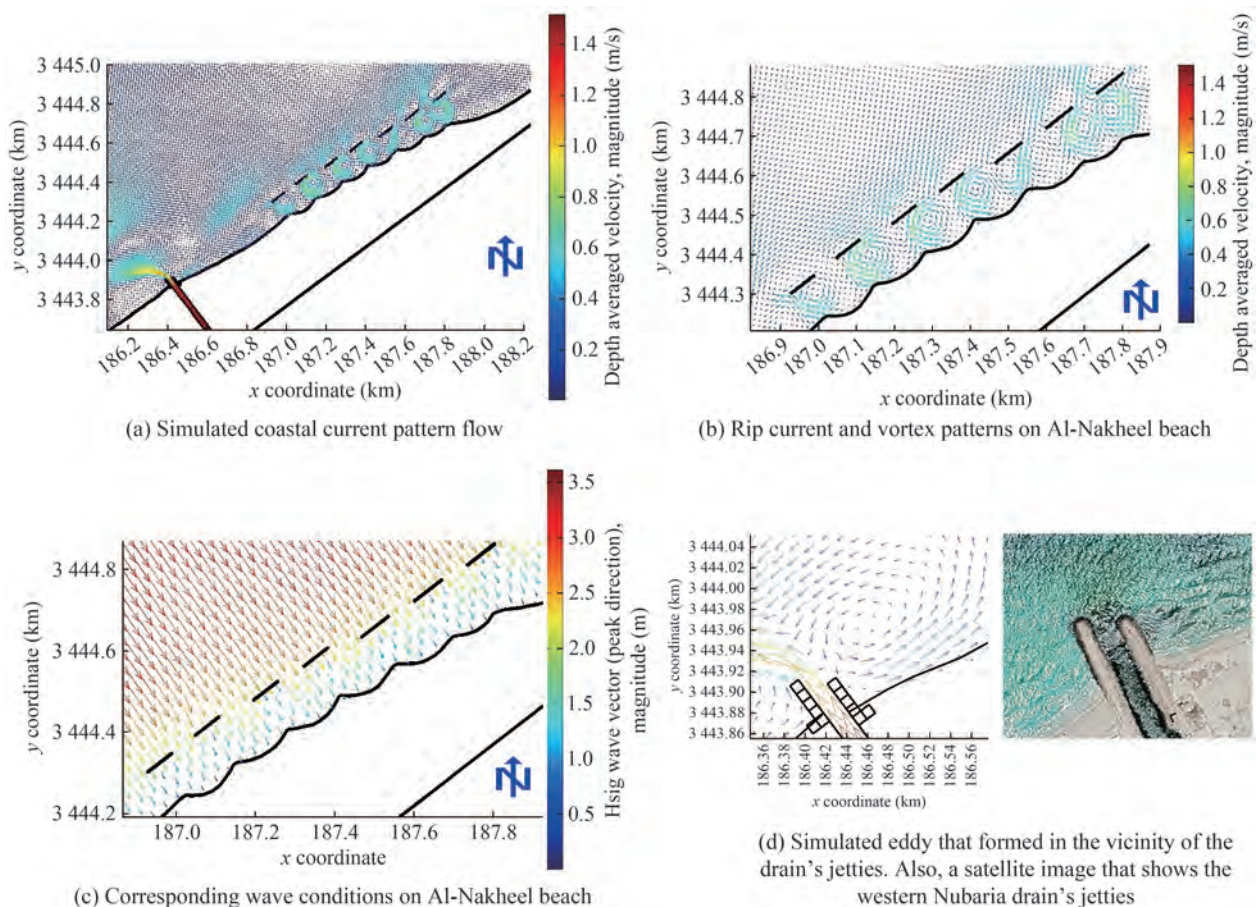


Figure 5 Simulated present situation at Al-Nakheel beach (Scenario 1)

form a pair of vortices behind them. Obliquely angled waves result in the formation of two opposite-direction longshore currents that act as feeders to rip currents. The velocities of rip currents and vortices reach 0.6 m/s in the swimming area. Such a velocity is dangerous for swimmers' lives. Moreover, a strong return flow extends 500 m offshore in the vicinity of the drain.

The spaces between the rip currents along Al-Nakheel beach vary from 68 m to 469 m, as shown in Figure 5. The model succeeds in illustrating the rip current behavior on the leeside of the structure. Some outputs display a duplication in the current speed through the root on the shore (leeside of breakwaters) to the rip head seaside. The larger waves create faster longshore currents, and peak current occurs when the wave approaches from an angle of 45° or more to the shoreline. Large significant wave heights with an angle of almost 45° to the shore generate longshore currents with a velocity of 1.2 m/s.

Wave propagation on the detached breakwaters generates flow vortices and a powerful return flow through the gaps between the structures. Within Al-Nakheel beach, the structurally controlled rip currents are generated under the effects of the detached breakwaters induced by bathymetric variations and alongshore hydrodynamic oscillations according to the rip classification of (Gallop et al. 2018).

4.2.2 Simulation of the situation of Al-Nakheel beach before breakwater construction (Scenario 2)

This scenario aims to check the effects of the breakwaters on the coastal hydrodynamic of the study area, especially the rip currents. The model is used to simulate the study area without breakwaters using the contour map of 2002. The scenario results reveal a limited rip current formation in magnitudes and repetitions, as displayed in Figure 6. The maximum rip current velocity is less than 0.4 m/s, and the rip current repetitions are less than a quarter of Scenario 1. In addition, a strong return flow occurs in the vicinity of the drain. Other wave conditions also induce limited rip currents. Rip current development is controlled by the coastline morphology and the hydrodynamic force mechanism (Iskander et al. 2021) or physical driving mechanism (Pitman et al. 2016). Clearly, the detached breakwaters increase the rip current risks within the study area.

4.3 Suggested solutions

4.3.1 What will happen if the sand deposits are removed? (Scenario 3)

A suggested solution by (SPA 2018; Iskander et al. 2021) is to remove the accumulated sand on the leeside of the detached breakwaters and use a floating fence. This suggestion is considered and implemented on the model with the same conditions mentioned in Scenario 1. The only change is to dredge the accumulated sand on the leeside of the breakwaters to reach the original morphology before the

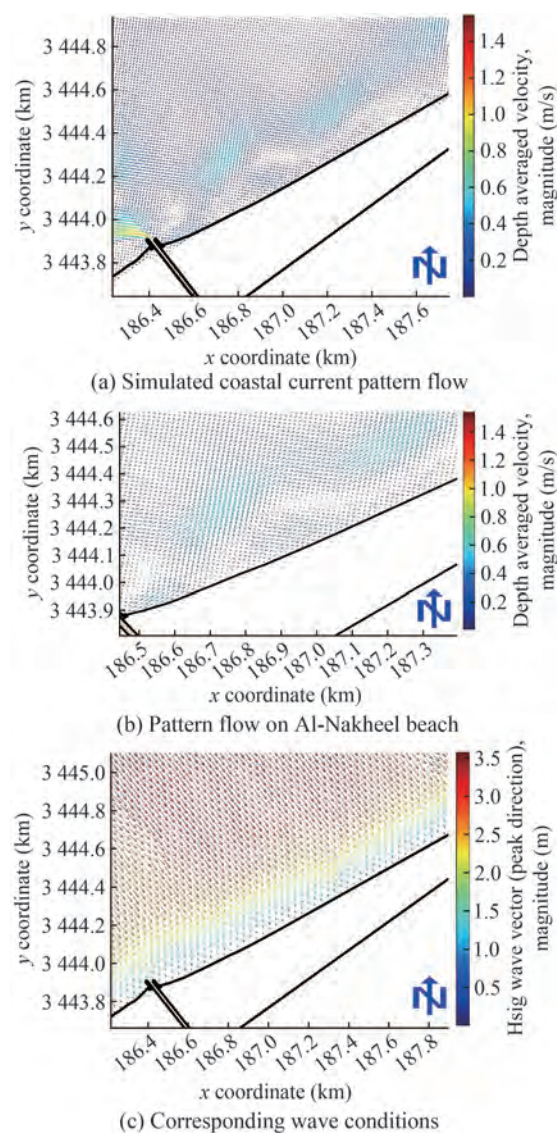


Figure 6 Simulated of Al-Nakheel beach without breakwaters (Scenario 2)

construction of the breakwaters. The results indicate that the same vortices are formed on the leeside of the structures but with fewer velocities near the shoreline. A relatively quiet area with an average width of 65 m with a rip current of less than 0.2 m/s near the shoreline exists, as shown in Figure 7(b). The implementation of this scenario needs the removal of 83476 m³ of sand, which costs about US\$453733.09. The extension of a floating fence with a length of 1000 m and a width of 65 m, which costs about US\$115775.97, leads to a total of US\$569509.06 for Scenario 3. This solution creates a safe area for swimming with a minor effect on the coastal hydrodynamic s such the waves and coastal currents.

4.3.2 What will happen if the gaps between the breakwaters are eliminated? (Scenario 4)

Scenario 4 simulates less discontinuity in the gaps by

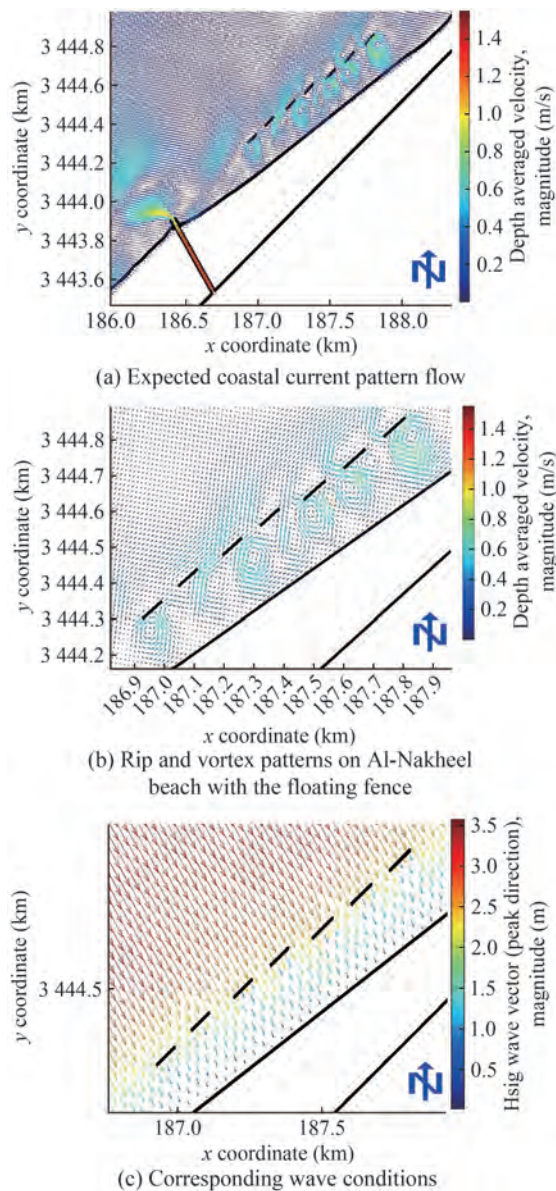


Figure 7 Simulation of the Al-Nakheel beach after removing the sand deposits (Scenario 3)

blocking the gap between every two adjacent breakwaters, apart from removing the sand deposits on the leeside of the breakwaters, as displayed in Figure 8. Scenario 4 costs about US \$4582369.50. The results show more powerful vortices and that the current velocity reaches 1.0 m/s.

4.3.3 What will happen if the discharge of the western Nubaria drain is stopped? (Scenario 5)

The construction of a drain at the boundary of Al-Nakheel beach complicates the problem. During some wave conditions, an eddy is formed in the vicinity of the drain, as shown in Figure 5(d). Reusing the drainage water of the Nubaria drain is one of the under-construction national projects. It is expected to stop the water from the Nubaria drain to the sea after construction. Scenario 5 simulates the

case of “no flow from the drain,” as displayed in Figure (9). The results clearly reveal a decrease in eddy velocity in the vicinity of the drain but no effect on the flow on the leeside of the breakwaters.

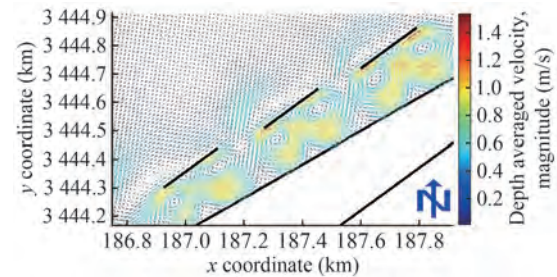


Figure 8 Result of Scenario 4 in the case of merging every two adjacent breakwaters

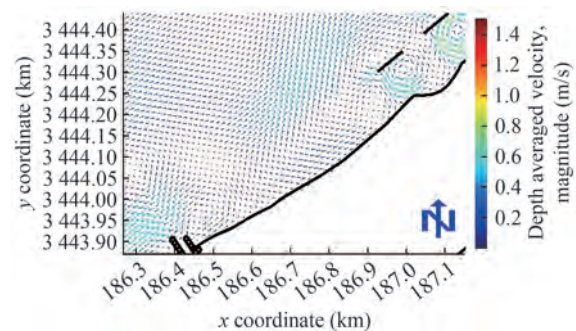


Figure 9 Result of Scenario 5 without flow from the drain

5 Conclusions and recommendations

Rip currents dominate the nearshore circulation system at Al-Nakheel beach, a summer resort in the northwest of Egypt. A remarkable increase in drowning cases has been recorded since the construction of seven detached breakwaters in 2003. The study aims to simulate rip currents and show the effects of detached breakwaters on rips using the Delft3D hydrodynamic model. The measured sea levels in 2013, wave datasets from 2015 to 2018, wind datasets in 2018, bed morphologies, and Google Earth satellite images from 2010 to 2020 are used to investigate the hydrodynamic behavior of the study area.

The predominant wind directions during the period and area of the investigation are NNW and WNW, with velocity ranges between 4 and 8.0 m/s. The NW wind induces waves perpendicular to the shoreline, which creates sets of hazard rip currents with a velocity reaching 0.6 m/s. The NE and SW wind enhances the formation of obliquely angled waves, which, in turn, induce longshore currents with a peaked velocity of 1.2 m/s.

The wave climate through considered wave data shows that the most wave direction from the deep water to the shallow water is the NW with (H_s) ranging from 0.50 m to

1.4 m on average. In addition, the propagation of regular waves on the detached breakwaters results in a decrease in the wave height on the leeside of the breakwaters. Consequently, the discontinuity in the breakwaters of Al-Nakheel beach causes a change in the pattern of the coastal currents. The nearshore circulation system at the Al-Nakheel beach comprises onshore flow, alongshore current, and temporary rip current in various patterns and forms.

Five simulation scenarios are applied using the Delft3D hydrodynamic model to identify the influences of the detached breakwaters on the rip currents along Al-Nakheel beach. Scenario 1 shows the recent situation at Al-Nakheel beach. Scenario 2 represents the condition of the beach before the breakwater construction. Scenario 3 illustrates the recommendation to remove the sand deposition behind the breakwaters. Scenario 4 shows how narrowing the gaps between breakwaters affects rip patterns. Scenario 4 simulates the study area with no flow from the Nubaria drain.

Based on different simulation scenarios, for controlling rip current hazards, dredging the salient formed on the leeside of the detached breakwaters and constructing a floating fence that extends about 65 m seaward are recommended to identify the suitable area for swimming on the leeside of the breakwaters.

Funding Supported by Egyptian Knowledge Bank (EKB)

Acknowledgement We sincerely thank Dr. Ahmed El-Kut, Coastal Research Institute, for his help and guidance in applying the hydrodynamical model. We are also grateful to Dr. Ahmed Magdy Khedr, Arab Academy for Science, Technology, and Maritime Transport, for his help.

References

- Benassai G, Aucelli P, Budillon G, De Stefano M, Di Luccio D, Di Paola G, Montella R, Mucerino L, Sica M, Pennetta M (2017) Rip current evidence by hydrodynamic simulations, bathymetric surveys and UAV observation. *Natural Hazards and Earth System Sciences* 17(9): 1493–1503. <https://doi.org/10.5194/nhess-17-1493-2017>
- Booij N, Ris RC, Holthuijsen LH (1999) A third-generation wave model for coastal regions: 1. Model description and validation. *Journal of Geophysical Research: Oceans* 104(C4): 7649–7666
- Castelle B, Coco G (2013) Surf zone flushing on embayed beaches. *Geophysical Research Letters* 40: 1–5. <https://doi.org/10.1002/grl.50485>
- Castelle B, McCarroll RJ, Brander RW, Scott T, Dubarbier B (2016) Modelling the alongshore variability of optimum rip current escape strategies on a multiple rip-channelled beach. *Natural Hazards* 81(1): 663–686. <https://doi.org/10.1007/s11069-015-2101-3>
- Ciarmiello M, Di Natale M (2016) Coastal erosion control. In: Kennish M.J. (ed.) *Encyclopedia of Estuaries*. Encyclopedia of Earth Sciences Series, Springer, Dordrecht. https://doi.org/10.1007/978-94-017-8801-4_386
- Dudkowska A, Boruń A, Malicki J, Schönhof J, Gic-Grusza G (2020) Rip currents in the non-tidal surf zone with sandbars: numerical analysis versus field measurements. *Oceanologia* 62(3): 291–308. <https://doi.org/10.1016/j.oceano.2020.02.001>
- Elkut AE, Taha MT, Zed ABEA, Eid FM, Abdallah AM (2021) Wind-wave hindcast using modified ECMWF ERA-Interim wind field in the Mediterranean Sea. *Estuarine, Coastal and Shelf Science* 252: 107267. <https://doi.org/10.1016/j.ecss.2021.107267>
- EPADP (2019) Ministry of water resources and irrigation. Public Authority for Drainage Projects
- Gallop SL, Bryan KR, Pitman SJ, Ranasinghe R, Sandwell DR, Harrison SR (2018) Rip current circulation and surf zone retention on a double barred beach. *Marine Geology* 405: 12–22. <https://doi.org/10.1016/j.margeo.2018.07.015>
- Holthuijsen LH (2007) *Waves in oceanic and coastal waters*. Cambridge University Press, Cambridge, United Kingdom, 24–29
- Iskander MM (2013) Wave climate and coastal structures in the Nile Delta coast of Egypt. *Emirates Journal for Engineering Research* 18(1): 43–57
- Iskander MM (2021) Stability of the Northern coast of Egypt under the effect of urbanization and climate change. *Water Science* 35(1): 1–10. <https://doi.org/10.1080/11104929.2020.1864255>
- Iskander MM, Frihy OE, El Ansary AE, El Mooty MMA, Nagy HM (2007) Beach impacts of shore-parallel breakwaters backing offshore submerged ridges, western Mediterranean coast of Egypt. *Journal of Environmental Management* 85(4): 1109–1119. <https://doi.org/10.1016/j.jenvman.2006.11.018>
- Iskander PN (2008) Sedimentological and morphological studies of the Northwestern Coast of Egypt (Alexandria-Abu Talat). Master thesis, Faculty of Science, Alexandria University, Alexandria, Egypt, 47–48
- Iskander MM, Hassan RM, Almaghraby MM, Abd-Almonem IM (2021) Overpopulation and rip current mitigation plan for the Egyptian coasts. *Cairo Water Week*, Cairo, Egypt, 1–10
- Khedr AM (2019) Sea level modeling and realization of lowest astronomical tide (LAT) for Alexandria Harbor, Egypt. PhD thesis, Arab Academy for Science, Technology and Maritime Transport, Alexandria, Egypt, 27–53
- Leatherman SP (2012) Rip currents: types and identification. *GSA Annual Meeting*, Denver, USA, 5–10. DOI: 10.1130/abs/2016AM-278408
- Mosetti F, Purga N (1990) Tides and sea level evolution at Alexandria, Egypt. *Il Nuovo Cimento* 13(3): 647–651. <https://doi.org/10.1007/BF02507628>
- Moursy ZA (1996) Sea temperature contribution to sea level at the South East sector of the Mediterranean. *Oebalia* 22: 131–137
- Nelson EW (1984) A simple and accurate method for calculation of the standard deviation of the horizontal wind direction. *Journal of the Air Pollution Control Association* 34(11): 1139–1140. <https://doi.org/10.1080/00022470.1984.10465866>
- Pitman S, Gallop SL, Haigh ID, Masselink G, Ranasinghe R (2016) Wave breaking patterns control rip current flow regimes and surfzone retention. *Marine Geology* 382: 176–190. <https://doi.org/10.1016/j.margeo.2016.10.016>
- Roth G (2018) Global burden of disease collaborative network. global burden of disease study 2017 (GBD 2017) results. Institute for Health Metrics and Evaluation (IHME), Seattle, USA. *The Lancet*, 392, 1736–1788. [https://doi.org/10.1016/S0140-6736\(18\)32203-7](https://doi.org/10.1016/S0140-6736(18)32203-7)
- Salama NM (2021) Application of a hydrodynamic model for simulation of water movement and sediment transport between Agami Headland and Sidi Krir, Alexandria, Egypt. Master thesis, Faculty of Science, Alexandria University, Alexandria, Egypt, 60–62
- Short AD (1985) Rip-current type, spacing and persistence, Narrabeen Beach, Australia. *Marine Geology* 65(1–2): 47–71. [https://doi.org/10.1016/0025-3227\(85\)90046-5](https://doi.org/10.1016/0025-3227(85)90046-5)
- SPA (2018) Hydrodynamic study for el Nakheel detached breakwater 21 km west of Alexandria. Shore Protection Authority, Alexandria, Egypt, National Water Research Institute Final technical report No. 20
- Williams JJ, Esteves LS (2017) Guidance on setup, calibration, and validation of hydrodynamic, wave, and sediment models for shelf seas and estuaries. *Advances in Civil Engineering* 2017: 1–25. <https://doi.org/10.1155/2017/5251902>
- Wright LD, Short AD (1984) Morphodynamic variability of surf zones and beaches: a synthesis. *Marine Geology* 56(1–4): 93–118